

Low Order Modeling of Combustion Instability Using a Hybrid Real/Ideal Gas Mixture Model

Paolo Maria Zolla^{*†}, Alessandro Montanari^{*}, Simone D'Alessandro^{*}, Marco Pizzarelli[‡] and Francesco Nasuti^{*}

^{*}*Sapienza University of Rome*

Via Eudossiana 18, 00184, Rome, Italy

[‡]*The Italian Space Agency (ASI)*

Via del Politecnico snc, 00133, Rome, Italy

[†]Corresponding author

Abstract

The present work focuses on the the state of development of a low-order numerical tool, specifically aimed to face combustion instability problems in liquid rocket engines employing shear coaxial injectors. Particular attention is focused on that kind of injectors, since they have been identified in the literature to have a central role in the high frequencies combustion instability dynamics. That is due to the passage of acoustic waves causing cyclic propellant pockets accumulation and release. In a low-order framework, flow field is computed using an Eulerian set of equations for three species, namely oxidizer, fuel, and combustion products mixtures.

In particular, the recent improvements involved the enhancement of the employed Equation of State, from the ideal one to a hybrid cubic one, in order to deal with cryogenic test cases. The hybrid EoS approach has been specifically developed to handle a mixture of ideal and real fluids, so that the typically cold oxidizer can be handled as a real fluid while the warmer species can be approximated as ideal gases. The combustion instability driving mechanism is regarded as a response function, which links acoustic waves to fuel mass flow rate oscillations, mimicking the described behavior of the coaxial injectors.

In order to predict the onset of transverse instabilities while keeping the computational load as low as possible, the chamber domain is discretized as 3D, whereas each of the injector domains as 1D. The one-dimensional tool handling the injectors can also be used as standalone, for dealing with longitudinal instabilities test cases, or in order to study the behavior of the single injector of a more complex system.

In the present work the most advanced results obtainable with the full 3D ideal gas model are presented, followed by the first analyses carried out with the hybrid-real fluid 1D model. The test case of interest is a cryogenic LOX/Methane engine prone to the onset of transverse instability.

1. Introduction

High frequency combustion instability (CI) is a major threat for liquid rocket engines. If instability occurs, severe pressure oscillations can be observed, and their amplitude can reach the order of magnitude of the mean chamber pressure [1–3], yielding to unexpected mechanical and thermal loads which might end up in the failure of the system.

Recent studies showed how both longitudinal and transverse instabilities developing in the combustion chamber might be related to a longitudinal dynamics taking place in the injectors, which show cyclic propellant pockets accumulation and release [2, 4, 5]. The reason for this might lie in the intrinsic nature of the commonly used shear coaxial injector. Such injector works with a radial density gradient supporting the fuel and oxidizer mixing. If some pressure oscillations onsets in the domain, waves travel longitudinally back and forth inside the elements, generating longitudinal pressure gradients. Perpendicularity between the two gradient vectors generates baroclinic torque, and vorticity in turn, at the recess location where propellant mixing happens. If upstream traveling pressure waves are strong enough, they might cause vortexes to intensify and the flow to slow down, entailing an O/F shift. Similarly, downstream traveling ones might push the mentioned vortexes suddenly towards the flame. The sudden heat release fluctuation caused by the mixture ratio variation, generates pressure oscillations in turn, potentially capable of closing a feedback loop between acoustics and heat release. If such a thermo-acoustic coupling takes place, combustion instabilities arise. Thus, it is straightforward to understand that well reproducing wave propagation inside the oxidizer post is mandatory to capture the characteristic times of the mentioned phenomenology.

To better understand and improve prediction capabilities, the scientific community studies such kind of instability with a joint effort of experimental tests and numerical models. As far as experiments are concerned, since full-scale tests are usually not affordable, lab-scale combustors [6–9] represent a cheaper alternative, allowing to get some results in a relatively short time. Regarding numerical simulations instead, different approaches with different goals are available, namely high-fidelity simulations and low order models. The former, consist in solving the flowfield with a highly detailed physics, including fluid dynamics and chemical kinetics: this class of calculations [4, 10, 11] require huge computational efforts. On the other hand, low order models involve the development of simplified tools capable of capturing some specific features of the investigated phenomenon [12–14]. Since such approaches are based on a simplified physics of the problem, suitable additional models are required, i.e. the so called “response functions”. Unfortunately, the presence of such additional models often implies preliminary tuning with experimental or numerical data.

Different methods have been explored over the years to obtain such response functions, such as the calibration based on either experimental data or high fidelity simulations [14, 15], or the derivation of some law from fundamental principles [16]. Despite all the efforts carried out so far in the literature, predictive capability of high frequency combustion instability has not yet been achieved with any numerical tool. Its a-priori prediction by means of a low-order model would lead to a significant reduction of expensive experimental tests and high-fidelity simulations, certainly impacting in a favorable way the development costs of new LREs.

In this paper, the prediction of spontaneous self sustained combustion instabilities is tackled using a non-linear reduced order Eulerian model, where the response function is designed to link pressure oscillations to fuel mass flow rate (instead of directly linking pressure waves to heat release), independently from any external data. This approach is capable to capture the aforementioned characteristics of the shear coaxial injector [17, 18], where the presence of acoustic waves is associated to the accumulation and release dynamics of the propellant pockets, inside the element. Also, to correctly reproduce acoustic propagation in the real fluid regimes typically found in LREs oxidizer posts, a newly developed hybrid real/ideal model is embedded in the solver.

This paper is structured as follows: first, in Section § 2, the numerical tool’s modeling is discussed, presenting its governing equations (§ 2.1), response function (§ 2.2), employed gas model (§ 2.3), and multi-dimensional approach (§ 2.4). Secondly, a test case prone to develop spontaneous transverse combustion instability is introduced in Section § 3, presenting in detail the experimental setup. Lastly, in Section § 4, the discussed numerical tool is tested. Obtained results are presented in the first place in a 3D framework with a fully ideal gas model (§ 4.1), and then in a one-dimensional framework with the newly developed hybrid real/ideal model (§ 4.2).

2. Modeling approach

Keeping in mind that the flow inside coaxial injectors can be assumed to be substantially one-dimensional (1D), this paper proposes the approach of dividing the domain in two zones, namely the injection plate, where each injector is handled by a one-dimensional solver, and the chamber, handled by an existing, already validated in-house software [19] for three-dimensional multi-species flows. For the sake of conciseness, this paper describes only the more interesting one-dimensional modeling, where both the real fluid model and response function are embedded. Description of the three-dimensional solver is omitted, since it is based on the well-known 3D ideal Eulerian model.

2.1 Governing equations

The one-dimensional solver implements a finite volumes Godunov-like numerical scheme, with a second order accuracy in both space and time. Governing equations for a quasi-one-dimensional (Q1D, one-dimensional domain with variable cross-section area) three-species Eulerian flow are assumed (subscript “ox” for oxidizer, “f” for fuel, and “p” for combustion products). The system of equations, in conservative form, can be written as [20]:

$$\begin{cases} (\rho A)_t + (\rho u A)_x = \dot{\omega}_{f1} & (1) \\ (\rho u A)_t + \left[(\rho u^2 + p) A \right]_x - p A_x = u \dot{\omega}_{f1} & (2) \\ (\rho A Y_{\text{ox}})_t + (\rho u A Y_{\text{ox}})_x = \dot{\omega}_{\text{ox}} & (3) \\ (\rho A Y_f)_t + (\rho u A Y_f)_x = \dot{\omega}_{f1} + \dot{\omega}_{f2} & (4) \\ (\rho e_0 A)_t + (\rho u h_0 A)_x = \dot{\omega}_{f1} h_{0,f} + \left(\dot{\omega}_{\text{ox}} \Delta h_{f,\text{ox}}^0 + \dot{\omega}_{f2} \Delta h_{f,f}^0 - \dot{\omega}_p \Delta h_{f,p}^0 \right) & (5) \end{cases}$$

where Y_{ox} and Y_f are mass fractions for oxidizer and fuel, e_0 and h_0 are, respectively, specific total energy and enthalpy, and $\Delta h_{f,i}^0$ is the standard formation enthalpy of the i -th species.

LOW ORDER MODELING OF COMBUSTION INSTABILITY USING A HYBRID REAL/IDEAL GAS MIXTURE MODEL

Fuel addition in the recess of the injectors is taken into account with:

$$\dot{\omega}_{f1} = \frac{\dot{m}_f}{l_f} \quad (6)$$

where l_f is the length of the fuel addition zone and \dot{m}_f is the fuel mass flow rate. The oxidizer mass flow rate \dot{m}_{ox} is instead forced at the inflow (left bound) along with the flow's total temperature T_0 .

The combustion process is represented by a single-step global reaction (in both the 1D and 3D solvers), which can be written, using an approximated Arrhenius form, as follows:

$$\dot{\omega}_{f2} = -G \frac{Y_{ox} Y_f}{\delta} e^{-T_r/T} \quad \text{if} \quad x > x_c \quad (7)$$

$$\dot{\omega}_{ox} = (O/F)_{st} \dot{\omega}_{f2} \quad (8)$$

$$\dot{\omega}_p = \dot{\omega}_{f2} + \dot{\omega}_{ox} \quad (9)$$

where δ and T_r are tuning parameters through which the heat release curve can be modified, G is the local mass flux, and x_c is the abscissa after which combustion is allowed to start. It must be underlined that the distance between the fuel injection location and x_c is representative of a space lag between the injection of the propellants in the chamber and their combustion, ideally representing atomization, evaporation, and mixing.

2.2 Response function

As previously mentioned, since the coupling mechanism between heat release rate and pressure oscillations which is driving the instabilities is missing, a so-called response function is needed. In order to mimic the behavior of the shear coaxial injectors, the fuel mass flow rate oscillations are linked to pressure oscillations as follows, as in [17, 18]:

$$\dot{m}_f = \dot{m}_{f,0} + \dot{m}'_f \quad (10)$$

$$\dot{m}'_f = \min \left[\hat{m}'_f, \frac{m_{f,acc}}{\delta t} \right] \quad \text{where} \quad \hat{m}'_f = \dot{m}_{f,0} \left[\exp \left(-\sigma \frac{p(t, x_s) - p_0(x_s)}{p_0(x_s)} \right) - 1 \right] \quad (11)$$

where \dot{m}'_f represents the fuel mass flow rate fluctuation caused by the passage of acoustic waves, σ is an amplification parameter, x_s is the abscissa where pressure is sampled, namely at the recess location, p_0 is the mean pressure at the sampling point (x_s), and $m_{f,acc}$ is the instantaneous fuel mass trapped into the vortex at the recess, introduced to ensure mass conservation, and computed as:

$$m_{f,acc} = - \int_0^t \dot{m}'_f dt \quad (12)$$

A typical behavior of the response function is shown in Figure 1, along with a sketch of a single injector one-dimensional domain. It can be seen how the fuel mass flow rate is reduced when high pressure hinders the passage of gaseous fuel, which is therefore accumulated in the recess. On the other hand, when the passage of acoustic waves creates a low pressure zone in the recess, the accumulated fuel is pushed into the chamber, eventually allowing mass flow rate to exceed its nominal value.

2.3 The hybrid real/ideal Equation of State

Thermodynamic states inside a liquid rocket engine might be very different among the different locations, even between injector elements and the core of the combustion chamber. Focusing on fuel and oxidizer at the injection domes, their thermodynamic state is always above their critical pressure, while not always above their critical temperature. Specifically, as mentioned before, oxidizer coming from either the tanks or the pumps is generally cold, and below its critical temperature, while fuel coming from the cooling jacket is generally hot and above its critical temperature. Lastly, downstream the ignition location, the combustion products temperature turns significantly higher than the critical temperature of the mixture. Thus, it is clear that to accurately reproduce acoustic propagation (fundamental for the prediction of CI), a real fluid model is needed.

For the mentioned reasons however, if a real fluid model is chosen, only the oxidizer is selected to be handled as a real fluid species, while fuel and combustion products are assumed to be ideal gas species, leading to a hybrid real/ideal gas model. Such assumption allows to significantly simplify the real fluid EoS. Therefore, starting from

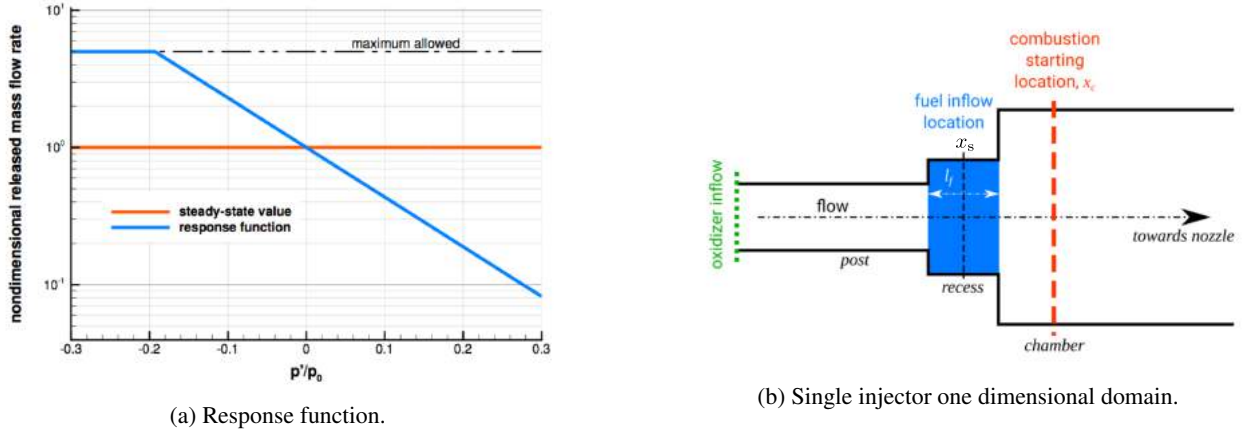


Figure 1: Typical behavior of the fuel mass flow rate with pressure according to the used response function (1a) and sketch of a common coaxial injector's Q1D domain (1b).

the original formulation by Kim et al. [21], it is possible to express the cubic Equation of State, specialized for the described mixture as:

$$p(\rho, T, \chi_i) = \frac{\rho R_u T}{w - \chi_{\text{ox}} b_{\text{ox}} \rho} - \frac{\chi_{\text{ox}}^2 a_{\text{ox}} \alpha_{\text{ox}}(T) \rho^2}{(w + \delta_1 \rho \chi_{\text{ox}} b_{\text{ox}})(w + \delta_2 \rho \chi_{\text{ox}} b_{\text{ox}})} \quad (13)$$

where ρ , p , T , w represent density, pressure, temperature and molar weight of the mixture, respectively, R_u is the universal gas constant, χ_{ox} the oxidizer's molar fraction, and $a_{\text{ox}} \alpha_{\text{ox}}(T)$, b_{ox} , δ_1 , δ_2 , are model parameters which are listed in [22].

The adoption of real fluid EoS implies the adoption of a proper Riemann Solver (RS) to solve the Riemann Problems at the interface between adjacent cells, suitable for generic multi-species flows, independent of any EoS. In the literature, a popular approximated RS is the Roe solver, whose original formulation [23, 24] was already extended to generalized EoS by Glaister [25]. Such a solver is re-derived with different primitive variables in [26], with respect to the original formulation, and implemented in the one-dimensional solver presented in this paper.

A complete determination of the thermodynamic quantities can be found in [27]. Validation of the implemented real fluid EoS against NIST data, for both pure fluids and mixtures, and validation of the Riemann solver against both ideal and real gas Riemann problems, can be found in [26, 28].

2.4 1D-3D integration

Integration between the 1D and 3D portions of the domain is handled as follows (see Figure 2): a certain surface \mathcal{B}_j at the left bound of the 3D domain is connected to the j -th injector. The flux vector is computed between the rightmost cell of the 1D domain and all the cells constituting the surface \mathcal{B}_j at the left boundary of the 3D domain. Then, the mass, x-momentum and energy fluxes are integrated over \mathcal{B}_j in order to be summed to the 1D cell. Since we assume axial flow coming from the injectors, and null average of v and w velocity components over \mathcal{B}_j potentially coming back from the chamber, the y- and z-momentum fluxes are neglected.

3. Experimental setup

The test case of interest has been conceived during a NASA program in 1989 (LOX/Hydrocarbon Combustion Instability Investigation Program, NAS3-24612 [29]) with the aim to evaluate the stability characteristics of the propellant combination LOX/CH₄ with respect to LOX/LH₂.

The engine of interest (class of 178 kN of thrust), in the following referred as NASA-LeRC (or simply "LeRC") design, is composed of a 14.38 cm diameter combustion chamber in which propellants are injected through a system of 82 shear coaxial injectors, where the oxidizer post measures 9.16 cm, while the recess 5.13 mm. The injectors are arranged in the faceplate in five concentric rows, where each row features equally spaced injectors (Fig. 3b). After the cylindrical portion of the chamber, whose length is 24.23 cm, a convergent-divergent nozzle extending for 14.32 cm and with a contraction ratio equal to 2.92 terminates the engine (Fig. 3a). Details of the thrust chamber assembly and injection plate can be seen in Figure 3.

LOW ORDER MODELING OF COMBUSTION INSTABILITY USING A HYBRID REAL/IDEAL GAS MIXTURE MODEL

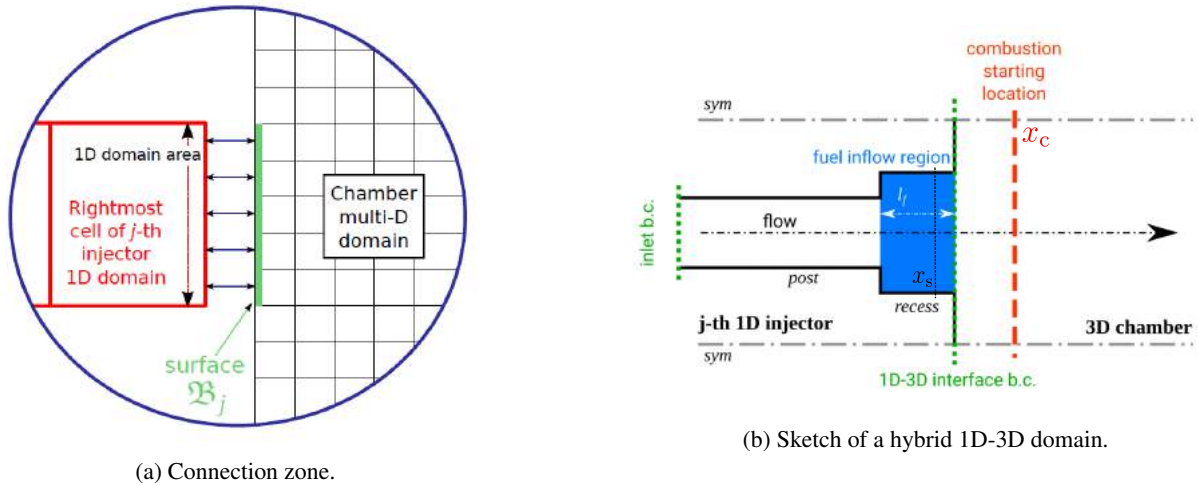


Figure 2: Domain splitting. Each injector is represented by a Q1D domain, while the chamber through a 3D one.

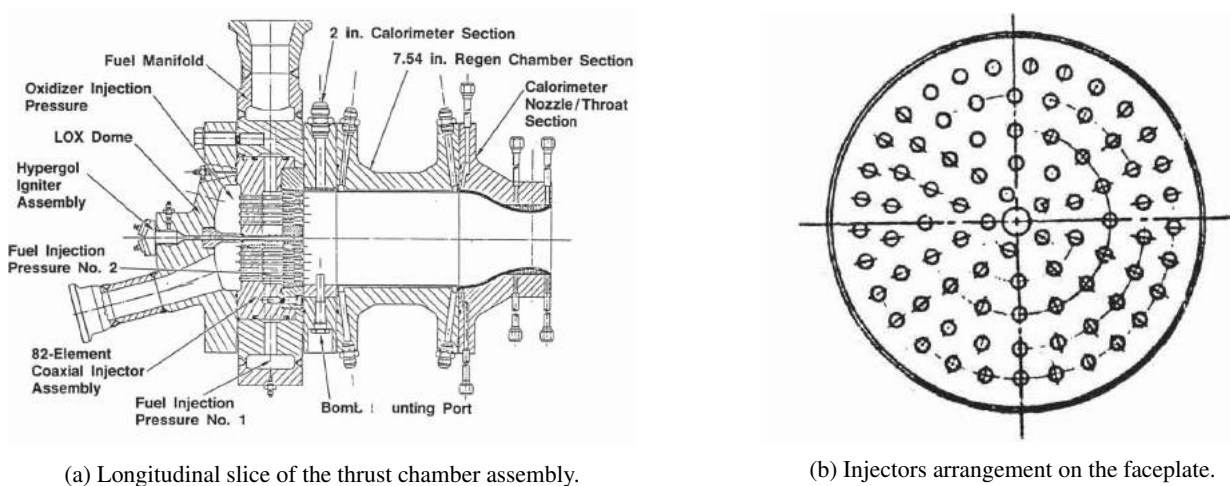


Figure 3: Details of the NASA-LeRC thrust chamber assembly and faceplate, from [29].

A total of 17 tests have been conducted in this program varying from case to case the combustor load point. In particular, the mixture ratio was varied in the range 2.5 – 3.7, hence employing in all cases a fuel-rich mixture, while the nominal chamber pressure was 13.8 MPa. Out of these 17 tests, six of them investigated spontaneous instability onset and, among these six tests, two resulted unstable during operations.

Table 1: Geometrical data of the NASA-LeRC combustor and details of the Test 014-004 load point.

Quantity	Value	Unit
Geometry		
Number of injectors	82	-
Post diameter	3.4	mm
Post length	91.6	mm
Recess diameter	5.71	mm
Recess length	5.13	mm
Chamber diameter	143.8	mm
Chamber length	242.3	mm
Throat diameter	84	mm
Contraction ratio	2.92	-
Nozzle length	143.2	mm
Operating conditions		
Nominal pressure	13.3	MPa
Mixture ratio	3.12	-
Oxidizer mass flow rate	30.9	kg/s
Fuel mass flow rate	9.9	kg/s
LOX Injection temperature	115.4	K
Gaseous CH ₄ injection temperature	275.4	K
Instability frequency	5200 (1T)	Hz
Instability peak-to-peak amplitude	20 (150% p_c)	MPa

In these tests, high amplitude activity has been triggered at the first tangential mode (1T) of the chamber (5.2 kHz). Indeed, the main cause leading to the trigger of the 1T mode was identified in [29] as an injection-coupled dynamics. Load point “Test 014-004” [29], is selected for the analyses. Complete information on the engine geometry and details of Test 014-004 are shown in Table 1.

4. Results

4.1 Hybrid 1D-3D analysis with ideal fluid model

The LeRC test case has been in the first instance approached using the ideal gas model, over the complete 1D-3D geometry. As previously mentioned in Section § 2.3, the use of ideal wave propagation velocities would introduce a significant error on the two-ways acoustic timing inside the oxidizer post. Thus, scaling the length of the oxidizer post is necessary to preserve the time needed by an acoustic wave to travel back and forth an injector. The scaling law can be expressed as:

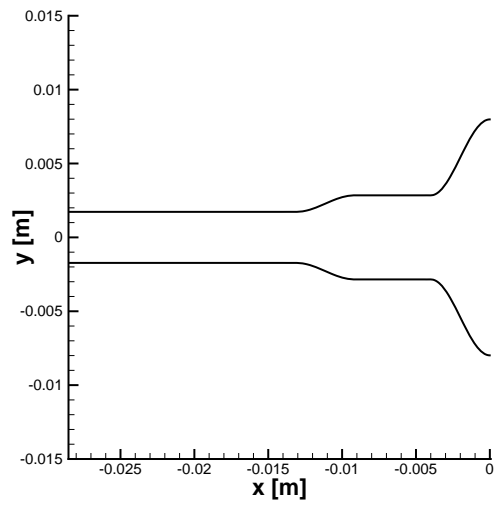
$$L_{inj} = L_{exp} \frac{a}{a_{exp}} \quad (14)$$

where, a_{exp} is the experimental speed of sound, and L_{exp} is the real length of the injector. The scaled post length, according to Equation (14), is 19.39 mm.

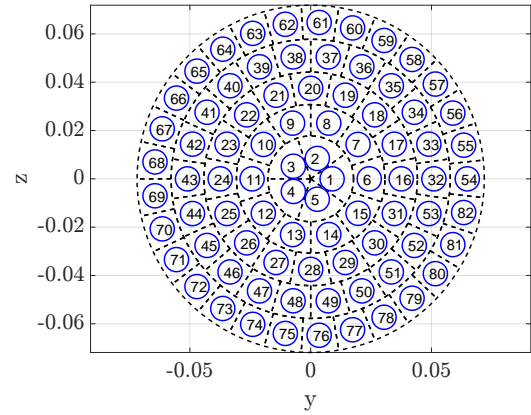
In the employed hybrid 1D-3D model, injectors are represented by 82 identical quasi-one-dimensional domains, each one featuring its own response function, discretized with 500 equally spaced cells and arranged on the faceplate equally spaced in 5 concentric rows. The combustion chamber is instead represented by a three-dimensional domain, using a five blocks mesh discretized in ~400k cells. Details of the domain discretization and of the injectors arrangement on the faceplate are shown in Figures 4 and 5.

Results are shown in Figures 6 through 9. Self-excited combustion instability is captured by the model. Chamber pressure is shown at 4 subsequent time frames, in Figures 6 and 7. As shown in Figure 6, the simulated instability

LOW ORDER MODELING OF COMBUSTION INSTABILITY USING A HYBRID REAL/IDEAL GAS MIXTURE MODEL



(a) Q1D geometry of a NASA-LeRC injector analyzed in a hybrid 1D-3D framework.



(b) Injectors arrangement on the faceplate.

Figure 4: Details of the NASA-LeRC injectors domain discretization.

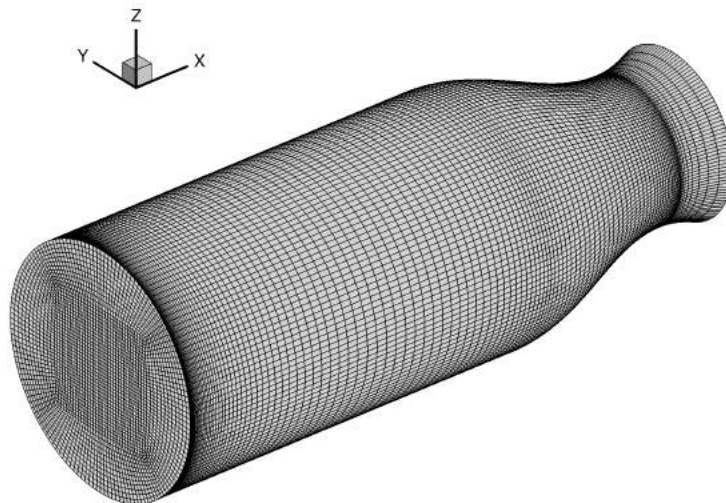


Figure 5: Details of the NASA-LeRC combustion chamber domain discretization.

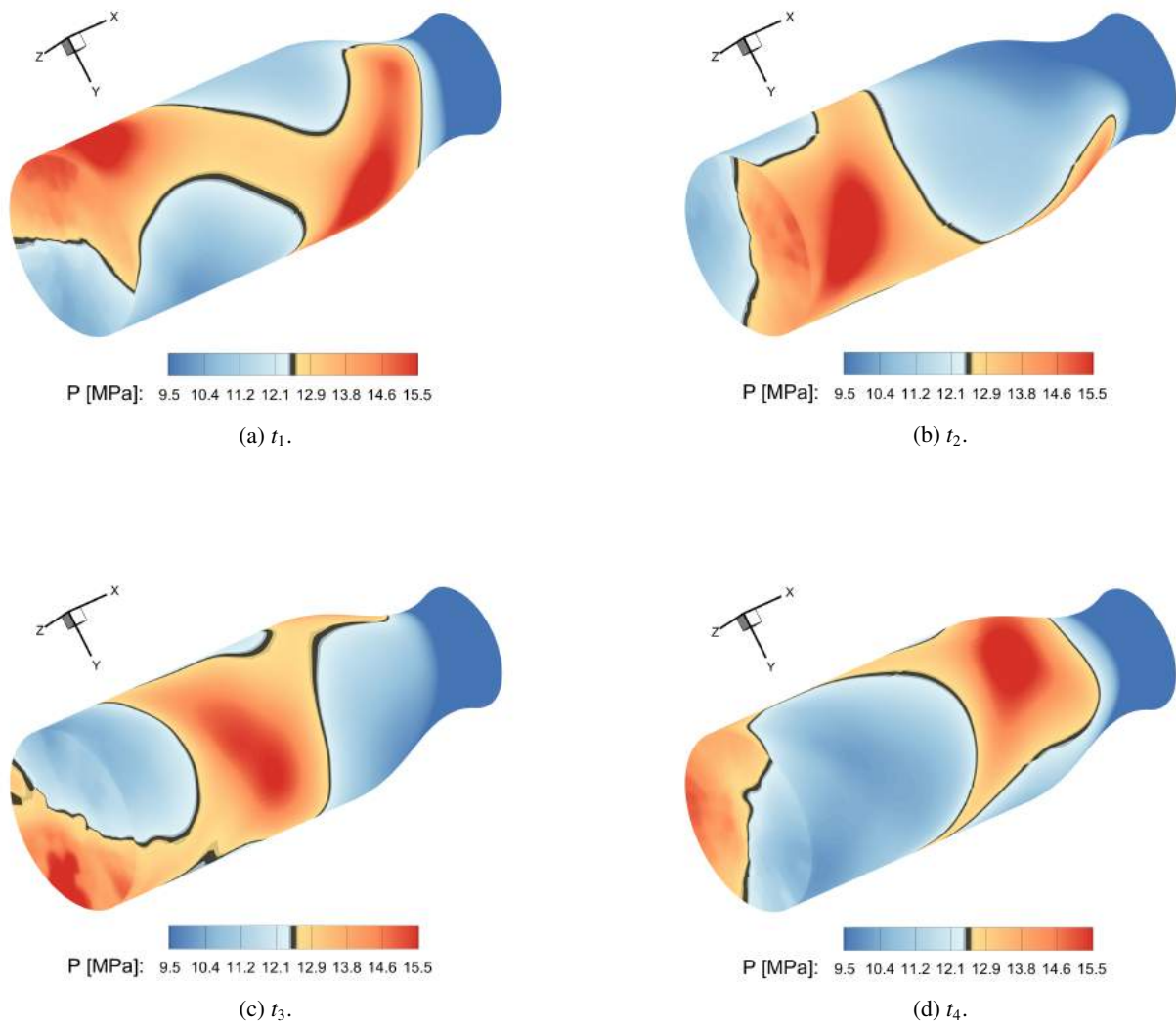


Figure 6: Chamber pressure in 4 subsequent temporal instants.

LOW ORDER MODELING OF COMBUSTION INSTABILITY USING A HYBRID REAL/IDEAL GAS MIXTURE MODEL

appears to be a 1T spinning mode at 5454 Hz, comparable with the experimental data in [29]. As can be seen from the field lateral view in Figure 7, the dynamics inside the injectors follows the rotating wave in the chamber, sustaining it. As the high pressure passes by an injector, a shockwave starts traveling upstream in it, causing a fuel accumulation in turn. As the wave reflects back at the boundary and comes back downstream, the accumulated fuel pocket is released. Such pocket is then convected to the combustion zone generating an heat release fluctuation. The timing of this hydro- and gas-dynamic is such that the instability loop closes.

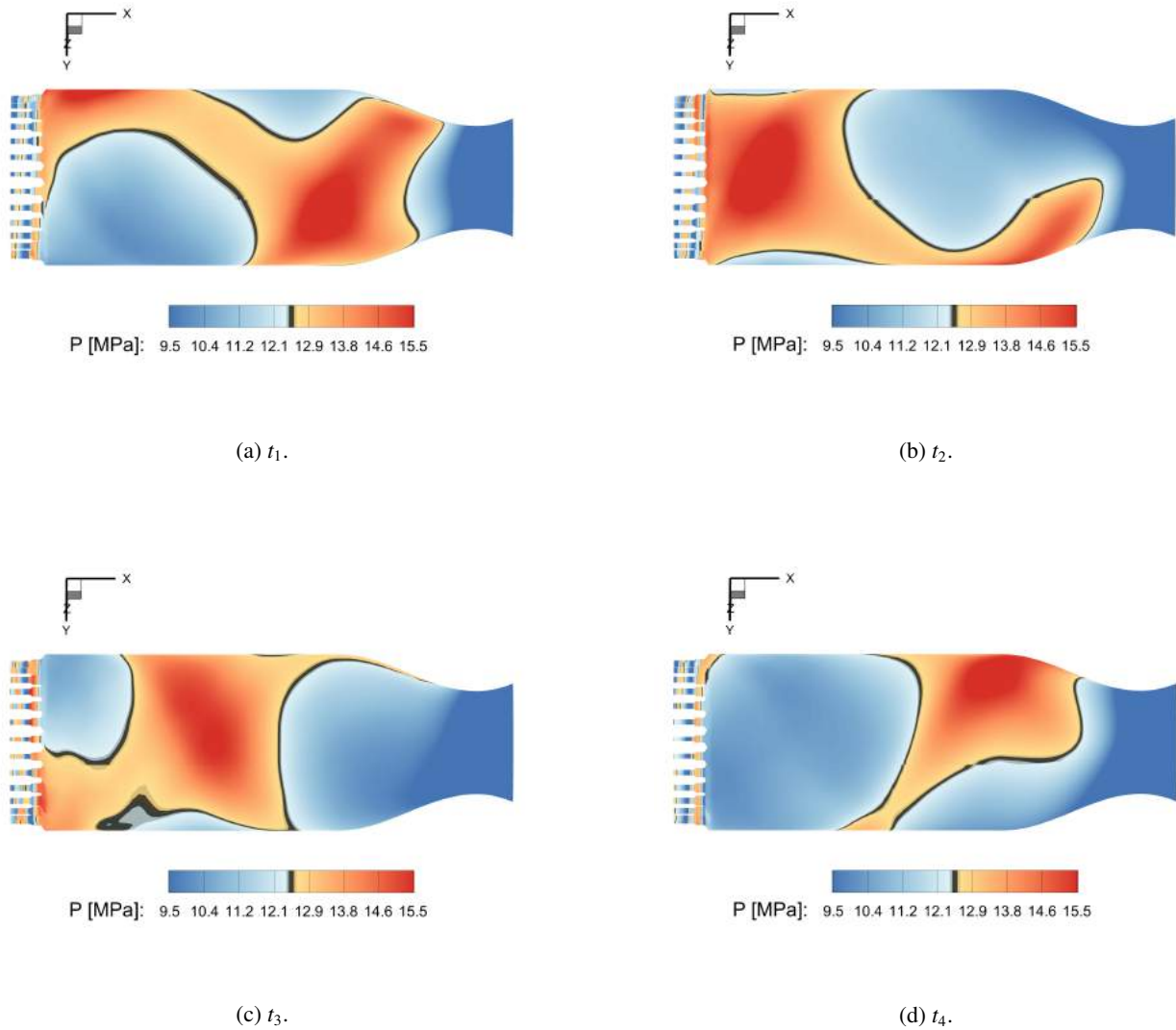


Figure 7: Chamber pressure in 4 subsequent temporal instants, lateral view with faceplate.

The dynamics of the accumulation and release of the fuel pockets is shown in Figure 8, where the temperature (8a) and the fuel mass fraction (8b) of the flowfield are shown. Temperature field is significantly heterogeneous in the chamber, since the 82 different response functions produce a significantly heterogeneous O/F ratio field instantaneously reaching the combustion zone.

Chamber pressure sampled at the outer edge of the faceplate is shown in Figure 9. As apparent, the typical evolution of a self-excited thermo-acoustic instability consists in an initial exponential growth followed by a limit cycle. It is interesting to notice how the pressure signal shown in Fig. 9c is quite smooth, typical of cylindrical geometries. Lastly, the power spectral density of the limit cycle pressure signal is shown in Figure 9d. The dominant frequency is 5454 Hz, which is in good agreement with the experimental data. A comparison between the experimental and computed characteristics of the instability limit cycle can be found in Table 2.

The hybrid 1D-3D solver with ideal fluid EoS has been able to correctly detect the onset of transverse CI in the examined test case, predicting with good accuracy the frequency of the limit cycle but committing a higher error

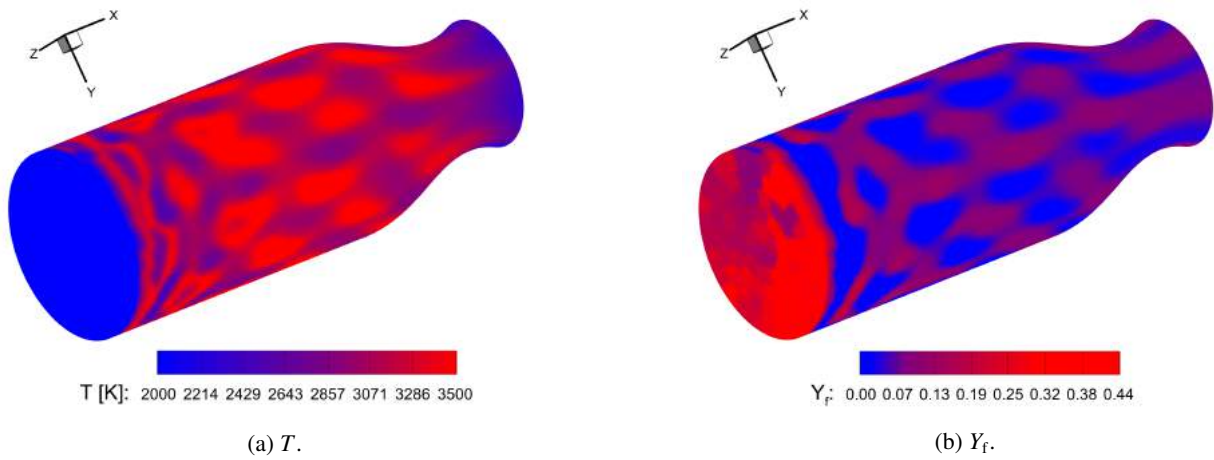


Figure 8: Chamber's temperature and fuel mass fractions.

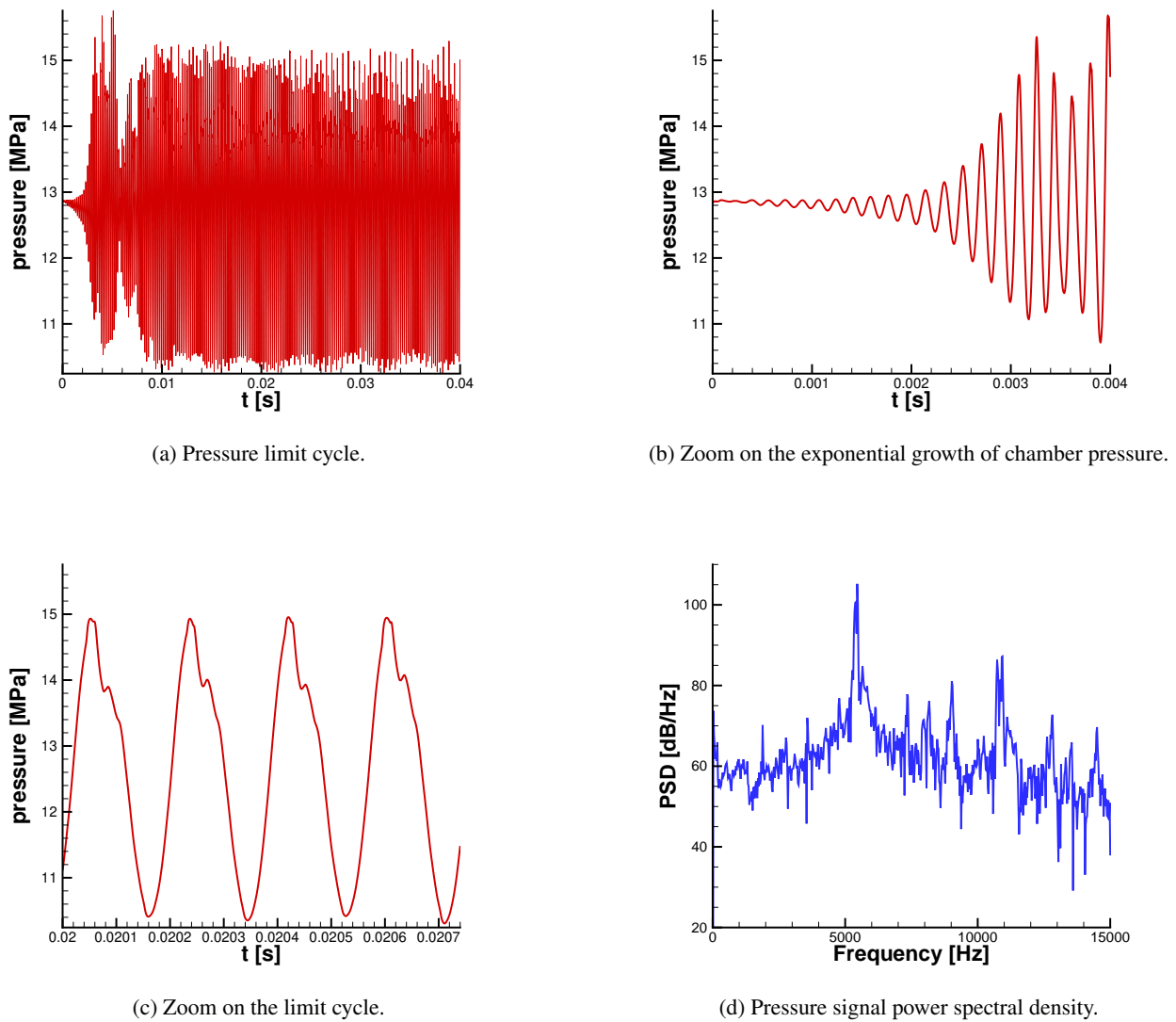


Figure 9: Computed chamber pressure sampled at the faceplate outer edge.

Table 2: Summary of the comparison between the obtained limit cycle and the experimental one (Test 014-004 [29]).

Quantity	Computed	Experimental	Error
Peak-to-peak amplitude	5.8 MPa	20 MPa	71%
Limit cycle frequency	5454 Hz	5200 Hz	<5%

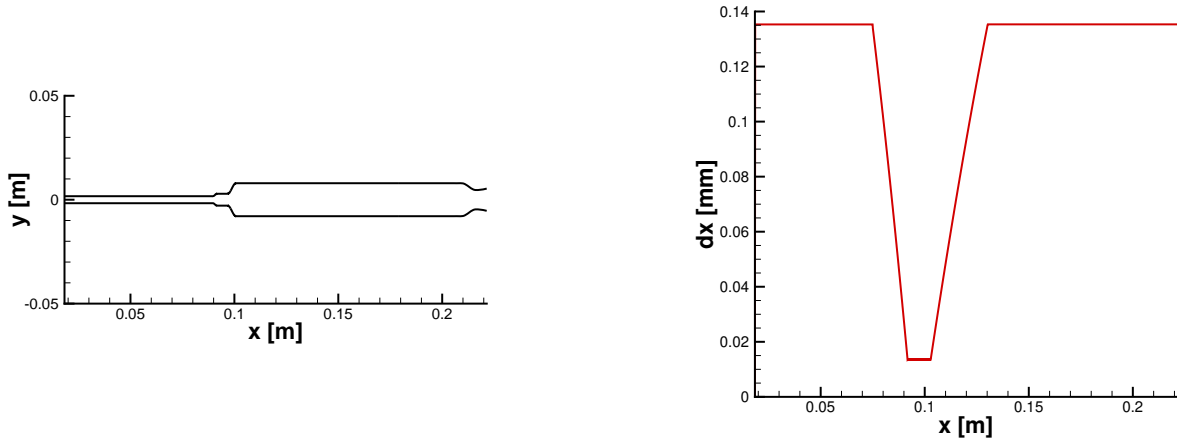
on the peak-to-peak amplitude. This discrepancy might be attributable to the ideal gas model, since the low flow compressibility might damp the pressure oscillations, in principle.

Furthermore, such a short down-scaled post might clash with the 1D assumption. The decision to switch to the more accurate hybrid real fluid model has been driven by the aforementioned two main reasons.

4.2 1D analysis with hybrid real/ideal fluid model

In the present section, the unstable dynamics of the NASA-LeRC engine is approached through the newly developed hybrid/ideal fluid model, in a quasi-1D fashion, as a preliminary step towards the analysis of the entire engine.

This modeling choice implies some geometrical modifications in order to reproduce the self-excited nature of the actual 3D multi-injector engine.



(a) Q1D geometry of a NASA-LeRC injector analyzed in a one-dimensional framework.

(b) Cell's length over the domain.

Figure 10: Details of the NASA-LeRC injector's Q1D domain analyzed in a one-dimensional framework.

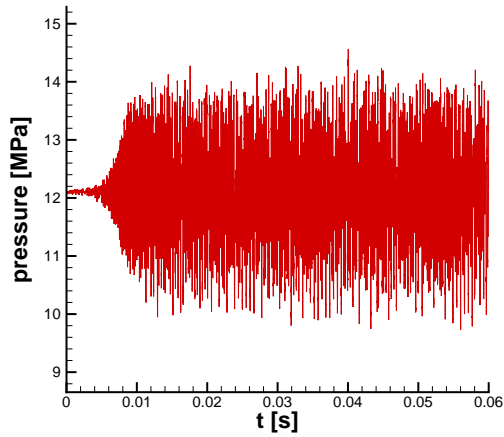
All of the injector dimensions are preserved including lengths and cross-section areas. Therefore, since only a single element out of the 82 is considered, the throat area has been down-scaled by a factor 82. The chamber diameter is consequently down-scaled to preserve the convergent nozzle contraction ratio.

Moreover, in order to capture transverse instabilities in a one-dimensional framework, the chamber length is scaled in order to have a first longitudinal mode (1L – numerical) frequency coinciding with the experimental 1T frequency. The chamber length scaling is operated assuming linear acoustics regime and a closed-closed cylinder geometry for the chamber.

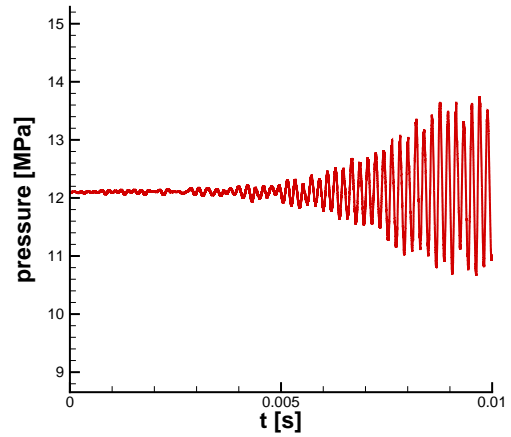
$$f_{1T,exp} = \frac{a_c}{2L_c} (1 - M_c^2) \quad (15)$$

where the subscript “c” means that the quantities are evaluated in the combustion chamber, a is the speed of sound, L is length, and M is the Mach number.

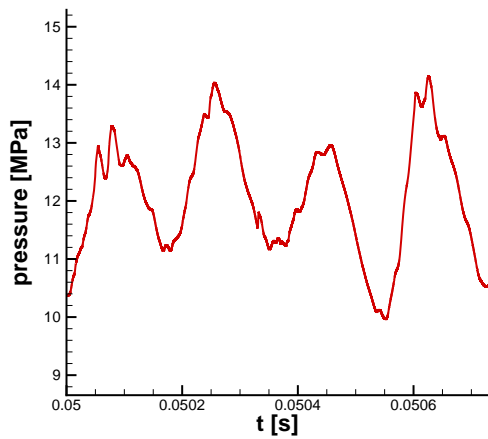
The domain is discretized in 2713 cells, which are no longer equally spaced in this case. Given the nature of the real fluid flow in the recess, a significant deceleration takes place there, causing a detrimental numerical diffusion for the convection of the fuel pockets. For this reason, a finer mesh is used in that zone. Details of the domain discretization are shown in Figure 10.



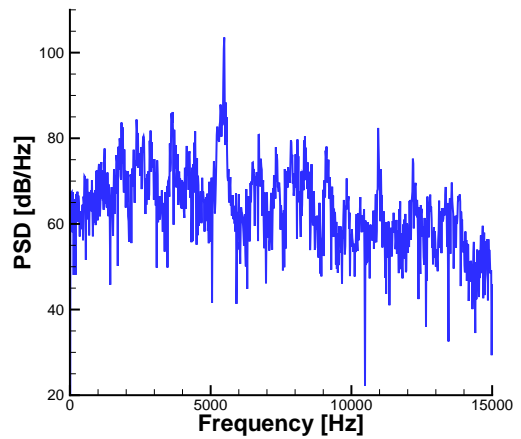
(a) Full pressure history.



(b) Zoom on the exponential growth of chamber pressure.



(c) Zoom on the limit cycle.



(d) Pressure signal power spectral density.

Figure 11: Computed chamber pressure sampled at the end of the chamber cylindrical section.

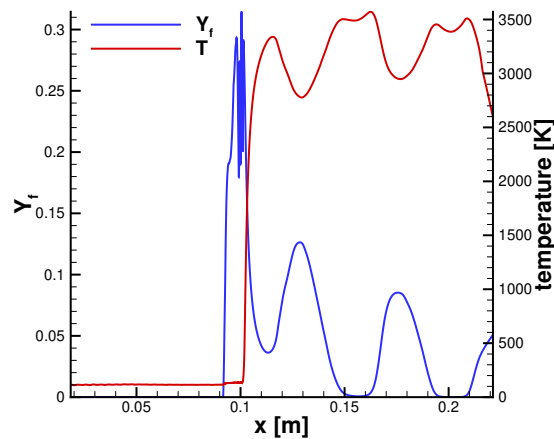


Figure 12: Dynamics of fuel mass fraction and chamber temperature during an instability.

Table 3: Summary of the comparison between the obtained limit cycle with the one-dimensional solver and the experimental one (Test 014-004 [29]).

Quantity	Computed	Experimental	Error
Peak-to-peak amplitude	4.8 MPa	20 MPa	76%
Limit cycle frequency	5483 Hz	5200 Hz	5.44%

Results are shown in Figure 11 and 12. It is clear from the figures how even in this case the low-order numerical tool is able to predict the occurrence of combustion instabilities. The pressure signal over time, sampled at the end of the chamber's cylindrical section, is shown in Figure 11a. The signal shows again an exponential growth of the amplitude of the oscillations (Fig. 11b), followed by a limit cycle (Fig. 11c). Power Spectral Density of the pressure signal is shown in Figure 11d.

The dynamics of the fuel pockets is reported in Figure 12 in terms of fuel mass fraction, as well as its influence on the chamber temperature. It is clear from the Figure how the cyclic accumulation and release of fuel pockets yields to the alternation between zones where the fuel is completely depleted with fuel-rich ones. Being the mixture nominally fuel-rich, temperature shows a decrease where a stronger fuel dilution occurs. This behavior leads to unsteady heat release, closing the instability feedback loop.

The predicted instability has the modal shape of the first longitudinal mode of the chamber (1L), with a peak-to-peak amplitude of 4.8 MPa and a dominant frequency of 5483 Hz. A comparison between the experimental and computed characteristics of the instability limit cycle can be found in Table 3.

As shown in the table, also in this case the accuracy in terms of the frequency of the limit cycle is good, while a higher discrepancy on the peak-to-peak amplitude is reported, despite the adoption of a real fluid simplified model. Such behavior might be in this case attributable to the lack of interaction among the different injector elements. Nevertheless, the injector model functionality in terms of response function dynamics is confirmed.

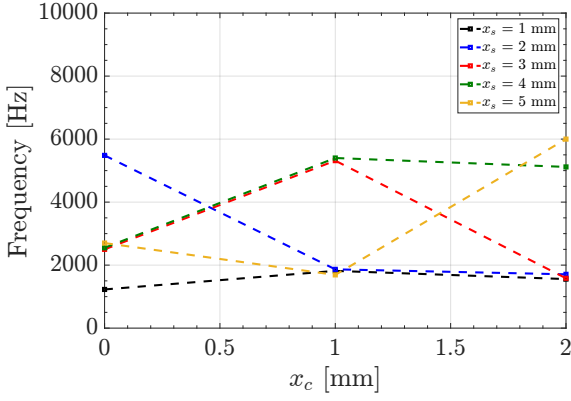
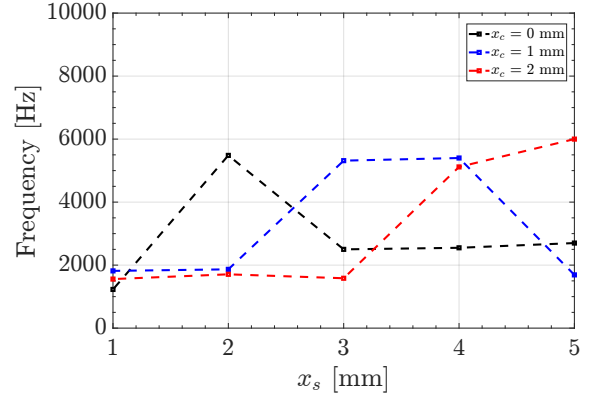
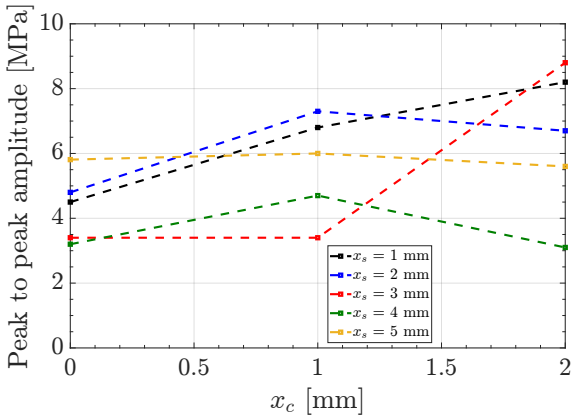
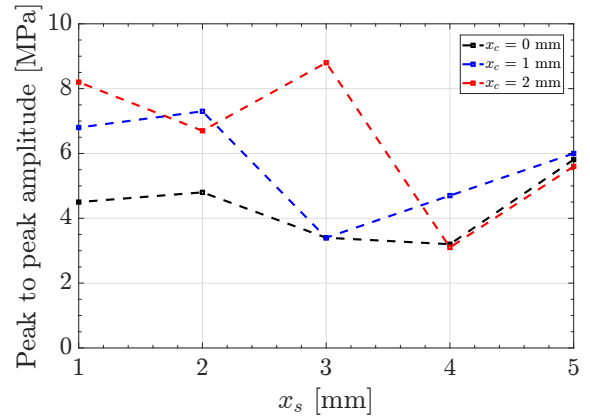
4.2.1 Sensitivity analyses on the main response function calibration parameters

In order to assess the effect that the free parameters x_c and x_s , appearing in the low-order model, have on the solution, a parametric analysis is carried out in this framework.

A strong dependency of both peak-to-peak amplitude and frequency on these two parameters in an ideal gas framework has already been discussed in [30]. This behavior is expected, since the distance between the two abscissas constitutes a space/time lag between pressure oscillations and unsteady heat release, therefore capable of modifying the overall unstable behavior. To assess their role in the present test case, different configurations are considered, with x_c equal to 0, 1, or 2 mm (from the faceplate), and x_s equal to 1, 2, 3, 4, or 5 mm (from the backstep).

In Figure 13 the results obtained are shown in terms of frequencies and peak-to-peak amplitude of limit cycles. Regarding the frequency, it can be stated that tuning the inquired parameters results in the presence of two dominant modes, one being the first longitudinal mode of the chamber (1L), at around 5200 Hz, and the other being the first

P. M. ZOLLA, A. MONTANARI, S. D'ALESSANDRO, M. PIZZARELLI, F. NASUTI

(a) Limit cycle frequency with respect to x_c for different values of x_s .(b) Limit cycle frequency with respect to x_s for different values of x_c .(c) Limit cycle peak-to-peak amplitude with respect to x_c for different values of x_s .(d) Limit cycle peak-to-peak amplitude with respect to x_s for different values of x_c .Figure 13: Limit cycle features for different configurations of x_c and x_s .

longitudinal mode of the entire system, at around 2000 Hz. The dynamic system shows therefore a strongly non-linear behavior where changes in the distance $x_c - x_s$ can lead to a bifurcation in the solution. Cycle amplitude also shows a strong dependency on the analyzed parameters, however a direct comparison is not possible in this case due to the different nature of the fluctuation spectra.

Despite this dependency of limit cycles features on (x_c, x_s) , the spontaneous instability is always captured, despite the significant simplifications embedded in the model.

5. Conclusions

In this work, a low-order approach for predicting spontaneous combustion instabilities in liquid rocket engines employing shear coaxial injectors modeling is presented and tested. In fact, those injectors present a peculiar longitudinal dynamics which has been identified to be responsible for the onset of combustion instabilities through the cyclic accumulation and release of propellant pockets.

The discussed numerical tool is tested against the NASA LeRC engine, a 178 kN LOX/Methane thrust chamber affected by self-excited combustion instability at some load points. Experimental data show the presence of self sustained transverse CI, with a peak-to-peak amplitude of 20 MPa and a dominant frequency of 5200 Hz.

This configuration is analyzed with both the complete 1D-3D solver with a fully ideal fluid model, and with the 1D solver with a hybrid real/ideal fluid EoS. In both cases, the reduced order numerical tool has been able to correctly detect the onset of spontaneous CI. The dominant frequency of the limit cycle has been either way predicted with good accuracy, with errors around 5% between the computed and experimental frequency. However, both solvers showed a higher discrepancy in the prediction of the peak-to-peak amplitude of the oscillations. Computed amplitude has been in both cases around 5 MPa, whereas the experimental amplitude is supposed to be 20 MPa according to the experimental

LOW ORDER MODELING OF COMBUSTION INSTABILITY USING A HYBRID REAL/IDEAL GAS MIXTURE MODEL

data available. This behavior is imputable in the case of the multi-dimensional solver to the employment of an ideal gas model which provides a significantly higher flow compressibility. In the case of the one-dimensional solver, instead, this lack of accuracy is supposed to be attributable to the forced reduction of a complex multi-injector dynamics to a single element one.

The one-dimensional solver with hybrid real/ideal gas model is at last used for a parametric analysis, with the aim of assessing the role of the low-order numerical tool most important calibration parameters, namely the incipient combustion abscissa x_c , and the pressure sampling abscissa x_s , used in the response function for the instability loop closure. The distance between the two points is in fact representative of a space/time lag between pressure oscillations and heat release, therefore capable of strongly influence the stability features of the system.

As expected, limit cycle frequencies and peak-to-peak amplitude appear to change significantly. If values of both x_c and x_s are changed even slightly, frequencies drift from the first longitudinal mode of the chamber (5200 Hz) to the first longitudinal mode of the system (2000 Hz), with peak-to-peak amplitudes varying from 3 to 9 MPa.

Ongoing and future perspectives foresee the analysis of the present test case in the multi-dimensional domain using the hybrid real/ideal fluid model.

Acknowledgments

This research was jointly funded by Sapienza University and the Italian Space Agency – Agenzia Spaziale Italiana (ASI) as part of the research N.2019-4-HH.0, project no. (CUP) F86C17000080005, carried out under the framework agreement N.2015-1-Q.0.

References

- [1] M. R. Orth, C. Vodney, T. Liu, W. Z. Hallum, T. L. Pourpoint, and W. E. Anderson, “Measurement of linear growth of self-excited instabilities in an idealized rocket combustor,” in *2018 AIAA Aerospace Sciences Meeting*, p. 1185, 2018.
- [2] S. Gröning, J. Hardi, D. Suslov, M. Oswald, and E. Kim, “Injector-driven combustion instabilities in a hydrogen/oxygen rocket combustor,” *Journal of Propulsion and Power*, vol. 32, pp. 560–573, May-June 2016. doi:10.2514/1.B35768.
- [3] Y. C. Yu, L. O’Hara, J. C. Sisco, and W. E. Anderson, “Examination of mode shapes in an unstable model rocket combustor,” 2009. 47th AIAA Aerospace Sciences Meeting Including the New Horizons Forum and Aerospace Expositions, 5-8 January, Orlando, Florida.
- [4] M. E. Harvazinski, C. Huang, V. Sankaran, T. W. Feldman, W. E. Anderson, C. L. Merkle, and D. G. Talley, “Coupling between hydrodynamics, acoustics and heat release in a self-excited unstable combustor,” *Physics of Fluids*, Vol. 27, 045102, 2015.
- [5] M. Wierman, N. Nugent, and W. E. Anderson, “Combustion response of a lox/lch4 element to transverse instabilities,” AIAA Paper 2011-5549, July 2011. 47th AIAA/SAE/ASEE Joint Propulsion Conference, San Diego, CA, doi:10.2514/6.2011-5548.
- [6] B. Pomeroy and W. Anderson, “Transverse instability studies in a subscale chamber,” *Journal of Propulsion and Power*, vol. 32, no. 4, pp. 939–947, 2016.
- [7] Y. C. Yu, J. C. Sisco, W. E. Anderson, and V. Sankaran, “Examination of spatial mode shapes and resonant frequencies using linearized euler solutions,” 2007. 37th AIAA Fluid Dynamich Conference & Exhibit, 25-28 June, Miami, FL.
- [8] S. Gröning, D. Suslov, M. Oswald, and T. Sattelmayer, “Stability behaviour of a cylindrical rocket engine combustion chamber operated with liquid hydrogen and liquid oxygen,” July 2013. 5th European Conference for Aeronautics and Space Sciences, Munich, Germany.
- [9] J. S. Hardi, M. Oswald, and B. B. Dally, “Study of lox/h2 spray flame response to acoustic excitation in a rectangular rocket combustor,” July 2013. 49th AIAA/ASME/SAE/ASEE Joint Propulsion Conference, San Jose, CA.

P. M. ZOLLA, A. MONTANARI, S. D'ALESSANDRO, M. PIZZARELLI, F. NASUTI

- [10] T. Schmitt, G. Staffelbach, S. Ducruix, S. Gröning, J. Hardi, and M. Oswald, "Large-eddy simulations of a sub-scale liquid rocket combustor: influence of fuel injection temperature on thermo-acoustic stability," 7th European Conference for Aeronautics and Space Sciences, July 2017, Milan, Italy.
- [11] A. Urbano, L. Selle, G. Staffelbach, B. Cuenot, T. Schmitt, S. Ducruix, and S. Candel, "Exploration of combustion instability triggering using large eddy simulation of a multiple injector liquid rocket engine," *Combustion and Flame*, Vol. 169, pp. 129-140, 2016.
- [12] R. Smith, M. Ellis, G. Xia, V. Sankaran, W. Anderson, and C. L. Merkle, "Computational investigation of acoustics and instabilities in a longitudinal-mode rocket combustor," *AIAA Journal*, Vol. 46, No. 11, November, 2008.
- [13] G. M. R. Tamanampudi, S. V. Sardeshmukh, and W. E. Anderson, "Study of combustion instabilities in transverse instability chamber using flame transfer functions," in *AIAA Propulsion and Energy 2019 Forum*, p. 4375, 2019.
- [14] L. T. W. Chong, T. Komarek, R. Kaess, S. Foller, and W. Polifke, "Identification of flame transfer function from les of a premixed swirl burner," 2010. ASME Turbo Expo 2010: Power for Land, Sea and Air, June 14-18, Glasgow, UK.
- [15] M. L. Frezzotti, S. D'Alessandro, B. Favini, and F. Nasuti, "Numerical issues in modeling combustion instability by quasi-1d euler equations," *International Journal of Spray and Combustion Dynamics*, vol. 0, no. 0, p. 1756827717711015, 2017.
- [16] W. A. Sirignano and P. P. Popov, "Two-dimensional model for liquid-rocket transverse combustion instability," *AIAA Journal*, Vol. 51, No. 12, pp. 2919-2934, 2013.
- [17] M. L. Frezzotti, S. D'Alessandro, B. Favini, and F. Nasuti, "Driving mechanisms in low order modeling of longitudinal combustion instability," American Institute of Aeronautics and Astronautics, 2018. AIAA Propulsion and Energy Forum, Cincinnati, OH, USA, 9-11 July.
- [18] S. D'Alessandro, *Low Order Modeling Approach to Longitudinal and Transverse Combustion Instability in Liquid Rocket Engines*. PhD thesis, Sapienza, Università di Roma, 2019.
- [19] M. L. Frezzotti, F. Nasuti, H. Cheng, and W. E. Anderson, "Extraction of response function from numerical simulations and their use for longitudinal combustion instability modeling," 2017. 55th AIAA Aerospace Sciences Meeting, Jan 9-13, Grapevine, TX, USA.
- [20] E. F. Toro, *Riemann solvers and numerical methods for fluid dynamics: a practical introduction*. Springer Science & Business Media, 2013.
- [21] S.-K. Kim, H.-S. Choi, and Y. Kim, "Thermodynamic modeling based on a generalized cubic equation of state for kerosene/lox rocket combustion," *Combustion and Flame*, vol. 159, no. 3, pp. 1351-1365, 2012.
- [22] G. Soave, "Equilibrium constants from a modified redlich-kwong equation of state," *Chemical engineering science*, vol. 27, no. 6, pp. 1197-1203, 1972.
- [23] P. L. Roe, "Approximate riemann solvers, parameter vectors, and difference schemes," *Journal of Computational Physics*, Vol. 43, pp. 357-372, 1981.
- [24] P. L. Roe and J. Pike, "Efficient construction and utilisation of approximate riemann solutions," in *Proc. of the sixth int'l. symposium on Computing methods in applied sciences and engineering*, VI, pp. 499-518, 1985.
- [25] P. Glaister, "An approximate linearised riemann solver for the euler equations for real gases," *Journal of Computational Physics*, vol. 74, no. 2, pp. 382-408, 1988.
- [26] S. D'Alessandro, M. Pizzarelli, and F. Nasuti, "A hybrid real/ideal gas mixture computational framework to capture wave propagation in liquid rocket combustion chamber conditions," *Aerospace*, vol. 8, no. 9, 2021.
- [27] S. I. Sandler, *Chemical, biochemical, and engineering thermodynamics*. John Wiley & Sons, 2017.
- [28] S. D'Alessandro, P. M. Zolla, M. Pizzarelli, B. Favini, and F. Nasuti, *A Hybrid Real/Ideal Gas Mixture Model in the Framework of Low Order Modeling of Combustion Instability*.
- [29] R. Jensen, H. Dodson, and S. Claffin, "Lox/hydrocarbon combustion instability investigation. final report," tech. rep., Rockwell International Corp., Canoga Park, CA (USA), 1989.

LOW ORDER MODELING OF COMBUSTION INSTABILITY USING A HYBRID REAL/IDEAL GAS MIXTURE MODEL

- [30] S. D'Alessandro, G. Fedeli, F. Tonti, J. Hardi, M. Oswald, B. Favini, and F. Nasuti, "Low-order modeling of combustion instability applied to cryogenic propellants," in *Proceedings of the 8th European Conference for Aeronautics and Space Sciences*, 2019.